


RESEARCH ARTICLE

The SLC26A9 inhibitor S9-A13 provides no evidence for a role of SLC26A9 in airway chloride secretion but suggests a contribution to regulation of ASL pH and gastric proton secretion

Sungwoo Jo¹ | Raquel Centeio² | Jinhong Park¹ | Jiraporn Ousingsawat² | Dong-kyu Jeon¹ | Khaoula Talbi³ | Rainer Schreiber² | Kunhi Ryu¹ | Kristin Kahlenberg³ | Veronika Somoza³ | Livia Delpiano⁴ | Michael A. Gray⁴ | Margarida D. Amaral⁵ | Violeta Railean⁵ | Jeffrey M. Beekman⁶ | Lisa W. Rodenburg⁶ | Wan Namkung¹ | Karl Kunzelmann² 

¹College of Pharmacy, Yonsei Institute of Pharmaceutical Sciences, Yonsei University, Incheon, South Korea

²Physiological Institute, University of Regensburg, Regensburg, Germany

³Leibniz Institute for Food Systems Biology at the Technical University of Munich, Freising, Germany

⁴Biosciences Institute, Faculty of Medical Sciences, Newcastle University, Newcastle upon Tyne, UK

⁵BioISI—Biosystems & Integrative Sciences Institute, Faculty of Sciences, University of Lisboa, Lisbon, Portugal

⁶Regenerative Medicine Utrecht, University Medical Center, Utrecht University, Utrecht, Netherlands

Correspondence

Wan Namkung, College of Pharmacy and Yonsei Institute of Pharmaceutical Sciences, Yonsei University, 85 Songdogwahak-ro, Yeonsu-gu, Incheon 21983, Republic of South Korea.
 Email: wnamkung@yonsei.ac.kr

Karl Kunzelmann, Physiological Institute, University of Regensburg, University street 31, Regensburg D-93053, Germany.
 Email: karl.kunzelmann@ur.de

Funding information

Deutsche Forschungsgemeinschaft (DFG), Grant/Award Number: DFG KU756/14-1; Gilead Sciences (Gilead), Grant/Award Number: Mucus in CF; UK CF-Trust, Grant/Award Number: SRC013

Abstract

The solute carrier 26 family member A9 (SLC26A9) is an epithelial anion transporter that is assumed to contribute to airway chloride secretion and surface hydration. Whether SLC26A9 or CFTR is responsible for airway Cl⁻ transport under basal conditions is still unclear, due to the lack of a specific inhibitor for SLC26A9. In the present study, we report a novel potent and specific inhibitor for SLC26A9, identified by screening of a drug-like molecule library and subsequent chemical modifications. The most potent compound S9-A13 inhibited SLC26A9 with an IC₅₀ of 90.9 ± 13.4 nM. S9-A13 did not inhibit other members of the SLC26 family and had no effects on Cl⁻ channels such as CFTR, TMEM16A, or VRAC. S9-A13 inhibited SLC26A9 Cl⁻ currents in cells that lack expression of CFTR. It also inhibited proton secretion by HGT-1 human gastric cells. In contrast, S9-A13 had minimal effects on ion transport in human airway epithelia and mouse trachea, despite clear expression of SLC26A9 in the apical membrane of ciliated cells. In both tissues, basal and

Abbreviations: ASL, airway surface liquid; CFTR, cystic fibrosis transmembrane conductance regulator; HCO₃⁻, bicarbonate; SLC26A9, Solute carrier family 26 member 9; TMEM16A, transmembrane member 16A; VRAC, volume regulated anion channel.

Sungwoo Jo and Raquel Centeio contributed equally to this work.

Wan Namkung and Karl Kunzelmann share senior authorship.

This is an open access article under the terms of the [Creative Commons Attribution-NonCommercial-NoDerivs](https://creativecommons.org/licenses/by-nc-nd/4.0/) License, which permits use and distribution in any medium, provided the original work is properly cited, the use is non-commercial and no modifications or adaptations are made.

© 2022 The Authors. *The FASEB Journal* published by Wiley Periodicals LLC on behalf of Federation of American Societies for Experimental Biology.

stimulated Cl^- secretion was due to CFTR, while acidification of airway surface liquid by S9-A13 suggests a role of SLC26A9 for airway bicarbonate secretion.

KEYWORDS

airways, asthma, Cl^- secretion, cystic fibrosis, pH regulation, S9-A13, SLC26A9

1 | INTRODUCTION

The epithelial anion transporter SLC26A9 (solute carrier 26 family member A9) is thought to contribute to hydration of the airway surface liquid (ASL) by operating as an Cl^- transporter.¹⁻⁷ A recent cryo-EM structure and functional analysis revealed that SLC26A9 operates as an uncoupled chloride transporter with a high turnover rate due to a rapid alternate-access mechanism.⁸ Biochemical properties, trafficking, and interaction between SLC26A9 and cystic fibrosis transmembrane conductance regulator (CFTR) are well noticed, but the true contribution of SLC26A9 to airway ion transport remains unclear. Although SLC26A9 operates as a Cl^- transporter rather than a Cl^- channel, it nevertheless produces substantial Cl^- currents that may contribute to basal airway Cl^- transport, that is, Cl^- transport under resting conditions in nonstimulated airway epithelial cells.^{4,9,10,11} Notably, in gastric parietal cells, SLC26A9 was shown to be relevant for acid secretion, probably by operating as a parallel Cl^- secretory pathway.⁶

CFTR and members of the SLC26A solute transporter family (SLC26A3,4,6,8,9) physically and functionally interact via R (regulatory) and STAS (sulfate transporter and antisigma factor antagonist) domains.^{4,12,13,14,15,16,17} Transport of bicarbonate (HCO_3^-) by SLC26A9 has been proposed by some scientists,^{3,18,19} but was not found by other laboratories.^{1,2,4,8} Loss of SLC26A9 was shown to alter intestinal HCO_3^- transport, acid secretion, and fluid absorption.^{5,6} SLC26A9 is inhibited by nonselective chloride channel inhibitors, including 4,4'-diisothiocyanatostilbene-2,2'-disulfonic acid (DIDS), NS3623, flufenamic acid, niflumic acid, and GlyH-101. However, these compounds inhibit a large range of Cl^- channels and showed a low potency and only partial inhibition of SLC26A9.^{1,2,4} Thus the lack of potent and selective inhibitors of SLC26A9 has hampered further investigations into the physiological function of SLC26A9.

In the present paper, we describe S9-A13, a highly potent and selective inhibitor of SLC26A9. Because we found no cross-inhibition of other SLC26 transporters or chloride channels, it was possible to analyze the contribution of SLC26A9 and CFTR to airway transport. While SLC26A9 does not contribute to airway Cl^- secretion, it controls ASL pH, probably by operating as a Cl^- /

HCO_3^- exchanger. However, in cells that do not express CFTR, SLC26A9 may operate as Cl^- transporter and may facilitate proton secretion in parietal cells.

2 | MATERIAL AND METHODS

2.1 | Identification of SLC26A9 inhibitors by high-throughput screening

A drug-like small-molecule library including 30 000 compounds was purchased from ChemDiv. (San Diego, CA, USA). Unless indicated otherwise, other chemicals were purchased from Sigma-Aldrich (St. Louis, MO, USA). Screening was performed in Ringer solution containing 140 NaCl, 5 KCl, 1 MgCl_2 , 1 CaCl_2 , 10 D-glucose, 10 HEPES (in mM; pH 7.4 with NaOH).

2.2 | Animals and treatments

Allergen challenge of mice has been described previously.²⁰ In brief, mice were sensitized to ovalbumin (OVA; Sigma-Aldrich, St. Louis, Missouri, USA) by intraperitoneal (ip) injection of 100 μg OVA in 100 μl aluminum hydroxide gel adjuvant (InvivoGen, San Diego, California, USA) on days 0 and 14. At days 21–23, mice were anesthetized (ketamine 90–120 mg/kg and xylazine 6–8 mg/kg) and challenged to OVA by intratracheal (it) instillation of 50 μg OVA in 100 μl saline. All animal experiments complied with the guidelines for animal research and were carried out in accordance with the EU Directive 2010/63/EU for animal experiments. Animal experiments were approved by the local Ethics Committee of the Government of Unterfranken/Wurzburg (AZ: 55.2.2-2532-2-1359).

2.3 | Cell culture and transfections

LN215 cells were cultured with Dulbecco Modified Eagle Medium (Welgene, Daegu, Korea) supplemented with 10% FBS, 100 U/ml penicillin, 100 $\mu\text{g}/\text{ml}$ streptomycin, 4 mM L-glutamine, and 1 mM sodium pyruvate. FRT

and CHO-K1 cells expressing ANO1, CFTR, or SLC26A4 were cultured using methods described previously.²¹ For SLC26A9 inhibitor screening and selectivity assays, LN215 cells expressing YFP-F46L/H148Q/I152L together with SLC26A3, SLC26A6, or SLC26A9 were generated by a lentiviral system containing the vectors pLenti6P.3-slc26a3, pLenti6P.3-slc26a6, and pLenti6P.3-slc26a9, respectively. Stable cell lines were selected using 1 µg/ml puromycin. Human embryonic kidney 293 (HEK293) cells were grown in DMEM media supplemented with 2mM L-glutamine. cDNA encoding human SLC26A9 with eGFP fused to its C-terminal was transfected in pcDNA3.1. Cells were transfected using standard protocols for Lipofectamine3000 (Thermo Fisher Scientific, Darmstadt, Germany). All media were supplemented with 10% heat-inactivated fetal calf serum (Capricorn Scientific, Ebsdorfergrund, Germany).

BCi-NS1 cells (kindly provided by Prof. R. Crystal, Weill Cornell Medical College, New York, USA) were cultured in supplemented bronchial epithelial cell growth medium (BEGM; Lonza, Basel, Switzerland). BCi-NS1 cells were grown on permeable supports for up to 30 days (Snapwell #3801, Corning, New York, USA) in an air/liquid interface (ALI). Human nasal cells were obtained from one adult donor using a cytological nasal brush and all procedures were ethically approved by the Institutional Medical Research Ethics Committee of the University Medical Centre, Utrecht (protocol ID: 16/586). The cells were expanded and fully differentiated as previously described.²² The human gastric tumor cell line HGT-1 was cultured as described earlier.²³

2.4 | RT-PCR and plasmids

For RT-PCR, total RNA from tissues or cells were isolated using NucleoSpin RNA II columns (Macherey-Nagel, Düren, Germany) and reverse-transcribed using random primer (Promega, Mannheim, Germany) and M-MLV Reverse Transcriptase RNase H Minus (Promega, Mannheim, Germany). Each RT-PCR reaction contained sense (0.5 µM) and antisense primer (0.5 µM) (Table 1), 0.5 µl cDNA, and GoTaq Polymerase (Promega,

Mannheim, Germany). After 2 min at 95°C, cDNA was amplified (targets 35 cycles, reference GAPDH 25 cycles) for 30s at 95°C, 30s at 56°C, and 1 min at 72°C. PCR products were visualized by loading on Midori Green Xtra (Nippon Genetics Europe) containing agarose. Primers are shown in Table 1.

2.5 | Cell-based high-throughput screening and YFP-fluorescence quenching

LN215 cells expressing YFP-F46L/H148Q/I152L and SLC26A9 were plated at a density of 25000 cells per well in 96-well microplates. Each well was washed two times with PBS (200 µl per well) and 50 µl of regular solution was added afterward. Test compounds were applied to each well at 25 µM and plates were incubated for 10 min at 37°C. The 96-well plates were transferred to a FLUOstar Omega Microplate Reader (BMG Labtech, Ortenberg, Germany) to measure SLC26A9 activity. Baseline fluorescence was recorded for 0.8 s, then 50 µl of NaI-substituted regular solution (140 mM NaI replacing 140 mM NaCl) was injected by a syringe pump. Fluorescence was recorded for 8 s. The initial slope of YFP fluorescence was used to analyze SLC26A9-mediated I⁻ flux rate. The YFP fluorescence quenching assay for assessment of SLC26A4, SLC26A6, SLC26A9, CFTR, ANO1, and VRAC activity were performed accordingly, as described in a previous study.²¹

2.6 | Cell viability assay

A Cell Titer 96® Aqueous One Solution Assay kit (MTS) (Promega, WI, USA) was used to determine the effect of compounds on cell viability. Calu-3 cells were cultured in 96-well plates in growth medium supplemented with 10% FBS for 24h until cell density reached ~40%. Cells were treated with S9-A13 and cisplatin for 24h followed by MTS analysis according to the supplier's protocol. The absorbance was measured by an Infinite M200 microplate reader (Tecan, Männedorf, Switzerland) at a wavelength of 490 nm.

TABLE 1 PCR primers

Gene accession number	Primer	Size (bp)
human SLC26A9 NM_052934.4	s: 5'-CTACATCATTCCTGACCTGC as: 5'-CTGCATGTGATACTTTTTGGG	724
mouse Slc26a9 NM_177243.4	s: 5'-CATTGCTGCGCTCTCTCAG as: 5'-CCTCTCTCCTGCTTCCGG	568
GAPDH NM_001289726	s: 5'-GTATTGGGCGCCTGGTCAC as: 5'-CTCCTGGAAGATGGTGATGG	200

2.7 | Immunoblots

Cells were lysed with RIPA buffer (Millipore, MA, USA) containing protease inhibitor cocktail. Each sample with equal amounts of protein was mixed with 5x SDS-sample buffer and then warmed to 37°C for 30 min. Eighty micrograms of protein samples were loaded to each lane, separated by 4–12% Tris Glycine Precast Gel (KOMA BIOTECH, Seoul, Korea) and then transferred into a PVDF membrane. PVDF membranes were blocked with 5% nonfat skim milk in Tris-buffered saline including 0.1% Tween 20 (TBST), by incubation for 1 h at room temperature and afterward incubating overnight at 4°C with the primary antibody for SLC26A9 (H00115019-A01; Abnova, Taipei City, Taiwan) and β -actin (Santa Cruz Biotechnology, Dallas, TX, USA). After incubation, the membranes were washed and incubated with HRP-conjugated anti-secondary IgG antibodies (Santa Cruz Biotechnology, Dallas, TX, USA) for 1 h at room temperature. SuperSignal™ Western Blot Substrate (Thermo Fisher Scientific, MA, USA) was used to visualize protein bands.

2.8 | Immunocytochemistry

Mouse lung sections were fixed using 4% paraformaldehyde (PFA) and 3.4% sucrose in PBS. Lung sections were deparaffinized with xylene and rehydrated through a series of ethanol. Cells grown on permeable inserts were fixed with 4% PFA in PBS and embedded in paraffin. Sections or cells were incubated with rabbit anti-SCL26A9 antibody (1:100, raised against mouse SCL26A9 aa 11–29, DRAAYSLSLFDDEFKDR, Davids Biotechnologie, Regensburg, Germany) overnight at 4°C. Nonspecific binding of the antibody to the airway epithelium was excluded in previous publications showing lack of binding in airways from patients carrying the F508del-CFTR/F508del-CFTR mutation, which causes a lack of apical expression of SLC26A9.²⁴ Antigen retrieval was performed in preheated Tris-EDTA buffer (pH 9.0) for 15 min, using a microwave before blocking. Cells were incubated with secondary anti-rabbit antibody conjugated with Alexa Fluor 488 or Alexa Fluor 546 (1:400) for 1 h at room temperature. Nuclei were counterstained with 5 μ M Hoe33342 (Thermo Fisher Scientific, Darmstadt, Germany). Section or cells were mounted with a fluorescence mounting medium (DAKO Cytomation, Hamburg, Germany). Immunofluorescence was examined with an Axio Observer microscope equipped with AxioCam 503 mono, ApoTome.2, and ZEN 3.0 (blue edition) software (Zeiss, Oberkochen, Germany).

2.9 | Patch clamp

Cells were patch clamped when grown on coated glass coverslips. Experiments were done at 37°C. Patch pipettes were filled with a cytosolic-like solution containing (in mM): KCl 30, K-gluconate 95, NaH_2PO_4 1.2, Na_2HPO_4 4.8, EGTA 1, Ca-gluconate 0.758, MgCl_2 1.03, D-glucose 5, ATP 3; pH 7.2. The intracellular (pipette) Ca^{2+} activity was 0.1 μ M. The bath was perfused continuously with Ringer's solution (in mM): NaCl 145, KH_2PO_4 0.4, K_2HPO_4 1.6, glucose 5, MgCl_2 1, Ca-gluconate 1.3 at a rate of 5 ml/min. In some experiments, extracellular chloride was substituted by equimolar concentrations of gluconate. Patch clamp experiments were performed as described previously.²⁵

2.10 | Transepithelial Ussing chamber recordings

BCi-NS1 and primary human airway epithelial cells polarized on permeable supports were measured under short-circuit conditions in non-perfused chambers with bicarbonate-buffered Ringer solution (mmol/l: NaCl 118.75; KH_2PO_4 0.4; K_2HPO_4 1.6; glucose 5; MgSO_4 1; Ca-gluconate 1.3, NaHCO_3 25; bubbled with 95% O_2 /5% CO_2). For measurements on mouse tracheas, animals were sacrificed by cervical dislocation, and freshly isolated tracheas were cleaned, opened, and measured in Ussing chambers under open circuit conditions. Methods have been detailed in previous reports.^{26,27}

2.11 | Intracellular pH measurements

For intracellular pH measurements cells were mounted and perfused with $\text{HCO}_3^-/\text{CO}_2$ solution (mmol/l: NaCl 118.75; KH_2PO_4 0.4; K_2HPO_4 1.6; glucose 5; MgSO_4 1; Ca-gluconate 1.3, NaHCO_3 25; bubbled with 95% O_2 /5% CO_2). Transport was stimulated with Cl^- free $\text{HCO}_3^-/\text{CO}_2$ solution bubbled with 95% O_2 /5% CO_2 . ΔpH was taken as a measure of $\text{Cl}^-/\text{HCO}_3^-$ antiport. Experimental procedures, acquisition of images, and data analysis were described recently.²⁶

2.12 | Airway surface liquid pH and assessment of proton secretory activity

Airway surface liquid pH (ASL pH) was measured using a temperature and CO_2 -controlled plate reader (TECAN SPARK 10 M), as previously described.²⁸ Briefly, the ASL was stained with 3 μ l of a mixture of dextran-coupled pH-sensitive pHrodo Red (0.5 mg/ml, λ_{ex} : 565 nm, λ_{em} :

585 nm, P10361, Thermo Fisher) and Alexa Fluor[®] 488 (0.5 mg/ml, λ_{ex} : 495 nm, λ_{em} : 519 nm, D22910, Thermo Fisher) diluted in glucose-free HCO_3^- KRB, overnight at 37°C, 5% CO_2 . For experiments, all chemicals were added to the basolateral bathing solution. pHrodo and Alexa Fluor[®] 488 were measured every 5 min, data were analyzed by subtracting the background values from each time point and then a ratio from pHrodo and Alexa Fluor[®] 488 was calculated. ASL pH standard calibration solutions were modified Ringer solution containing, in mM, 86 NaCl, 5 KCl, 1.2 CaCl_2 , 1.2 MgCl_2 , and either 50 MES (pH 5.5), 50 HEPES (pH 7.0), or 50 Tris (pH 8.0) at 37°C.

Proton secretory activity and corresponding data analysis were conducted by means of the pH-sensitive fluorescence dye 1,5 carboxy-seminaphtho-rhodafleur acetoxymethylester (SNARF-1-AM; Life Technologies), as described previously.²³

2.13 | Materials and statistical analysis

All compounds used were of highest available grade of purity. Data are reported as mean \pm SEM. Student's *t*-test (for paired or unpaired samples as appropriate) or ANOVA were used for statistical analysis. A *p*-value <.05 was accepted as significant difference. For each experimental series, the number of animals used and the number of measurements/assays/reactions is provided.

3 | RESULTS

3.1 | Identification of SLC26A9 inhibitor by high-throughput screening

For identification of novel small-molecule inhibitors for SLC26A9, a cell-based high-throughput screening was conducted using LN215 astrocytoma cells that were stably expressing human SLC26A9 and halide-sensitive yellow fluorescent protein (YFP-F46L/H148Q/I152L) (Figure 1A). LN215-SLC26A9-YFP cells were incubated in 96-well microplates for 24 h, and then treated with 25 μM of the test compounds for 10 min. Afterward, YFP fluorescence quenching by addition of iodide buffer was measured (Figure 1B). Representative YFP fluorescence traces and the effects of SLC26A9 inhibitors and inactive compounds are shown in Figure 1C,D. Screening of 30 000 drug-like small molecules revealed three novel chemical classes of SLC26A9 inhibitors: S9-A01, S9-B01 and S9-C01. S9-A01, S9-B01, and S9-C01 potently inhibited the Cl^-/I^- exchange activity of SLC26A9 in a dose-dependent manner with IC_{50} of 2.25 ± 0.52 , 16.63 ± 3.43 , and $38.00 \pm 1.88 \mu\text{M}$,

respectively (Figure 2A–D). In contrast, the CFTR-inhibitor GlyH-101 that has been reported to inhibit also SLC26A9 currents⁴ did not inhibit the Cl^-/I^- exchange activity of SLC26A9, even when applied at 100 μM (Figure 2E). Notably, S9-A01 blocked SLC26A9 activity more potently than other inhibitors. To improve potency of S9-A01, 17 derivatives of S9-A01 were generated of which S9-A13 inhibited SLC26A9 most potently with an $\text{IC}_{50} = 90.9 \pm 13.4 \text{ nM}$ (Table 2).

3.2 | Potent inhibition of SLC26A9-mediated anion exchange by S9-A13

The effects of S9-A13 on SLC26A9-mediated anion (Cl^-/I^- and Cl^-/SCN^-) exchange activities were measured in LN215-SLC26A9-YFP cells. S9-A13 potently inhibited SLC26A9-mediated Cl^-/I^- and Cl^-/SCN^- exchange activities with IC_{50} of $90.9 \pm 13.4 \text{ nM}$ and $171.5 \pm 34.7 \text{ nM}$, respectively (Figure 3A–D). To determine whether S9-A13 affects cell viability, MTS assays were performed on Calu-3 cells endogenously expressing SLC26A9. Cells were treated with S9-A13 up to a concentration of 10 μM . No cytotoxicity was observed for S9-A13 even at high concentrations of the inhibitor (Figure 3E).

3.3 | Selective inhibition of SLC26A9 by S9-A13

We examined potential effects of S9-A13 on other anion exchangers (SLC26A3, SLC26A4, SLC26A6), and chloride channels (CFTR, ANO1, and VRAC). However, even a high concentration (10 μM) S9-A13 did not affect the Cl^-/I^- exchange activity of SLC26A3 and SLC26A4 or Cl^-/SCN^- exchange activity of SLC26A6. At 10 μM S9-A13 did not alter chloride transport by CFTR, ANO1, or VRAC. In contrast, the Cl^-/I^- exchange activities of SLC26A3, SLC26A4, and SLC26A6 were significantly inhibited by DR_{inh} -A250, YS-01, and niflumic acid, while Cl^- transport by CFTR, ANO1, and VRAC was completely blocked by CFTR_{inh} -172, Ani9-5f, and DCPIB, respectively (Figure 4A–G).

3.4 | S9-A13 inhibits SLC26A9 but shows little effects on CFTR currents in HEK293 cells

HEK293 cells were transfected with SLC26A9-cDNA, which induced strong expression of SLC26A9 protein (Figure 5A,B). Partially membrane-localized SLC26A9 caused robust constitutive whole cell currents as detected by whole cell patch clamping, which were inhibited by

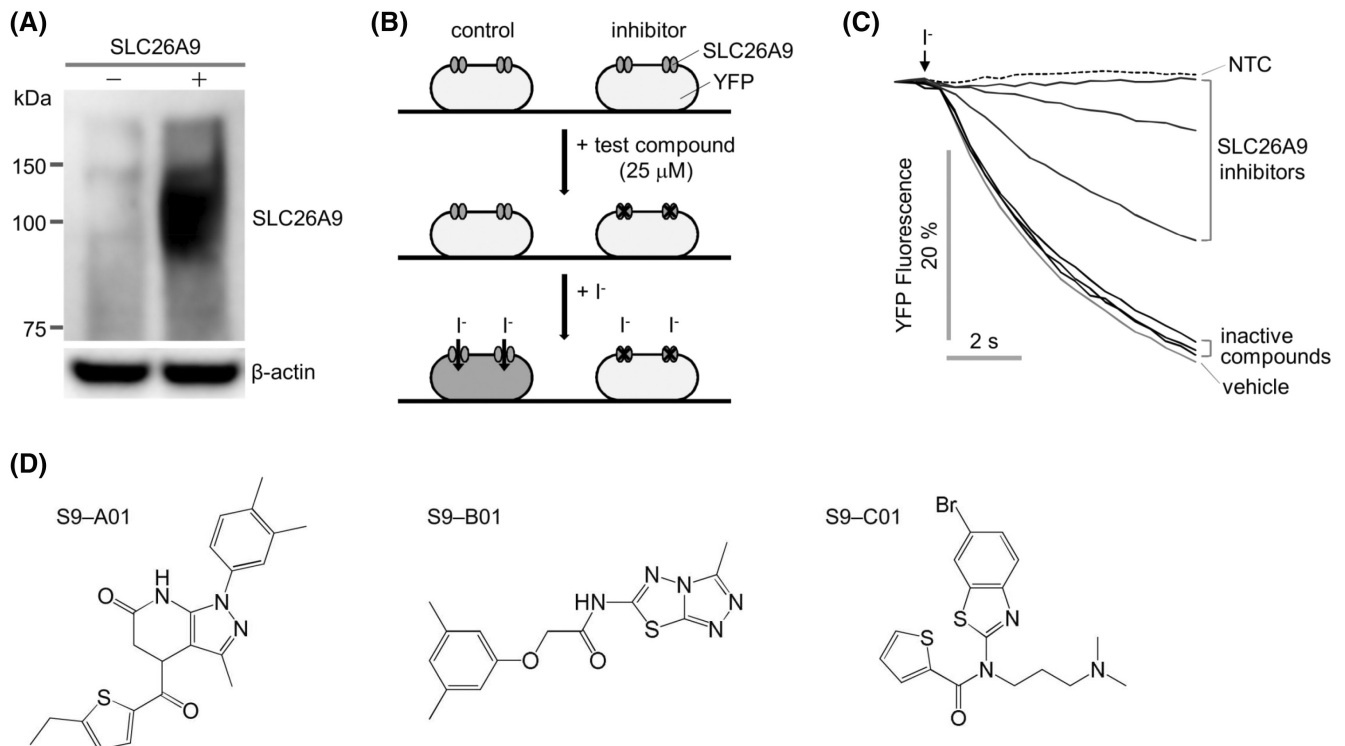


FIGURE 1 Identification of novel small molecule inhibitors of SLC26A9. (A) Immunoblot of SLC26A9 in LN215 and LN215-SLC26A9-YFP cells. (B) Schematic diagram showing the high-throughput screening process. (C) Representative YFP fluorescence traces of SLC26A9 inhibitors and inactive compounds in LN215-SLC26A9-YFP cells. Cells were treated with test compounds at 25 μ M for 10 min. (D) Chemical structures of three classes of SLC26A9 inhibitors. Non-transfected cells (NTC, dashed line).

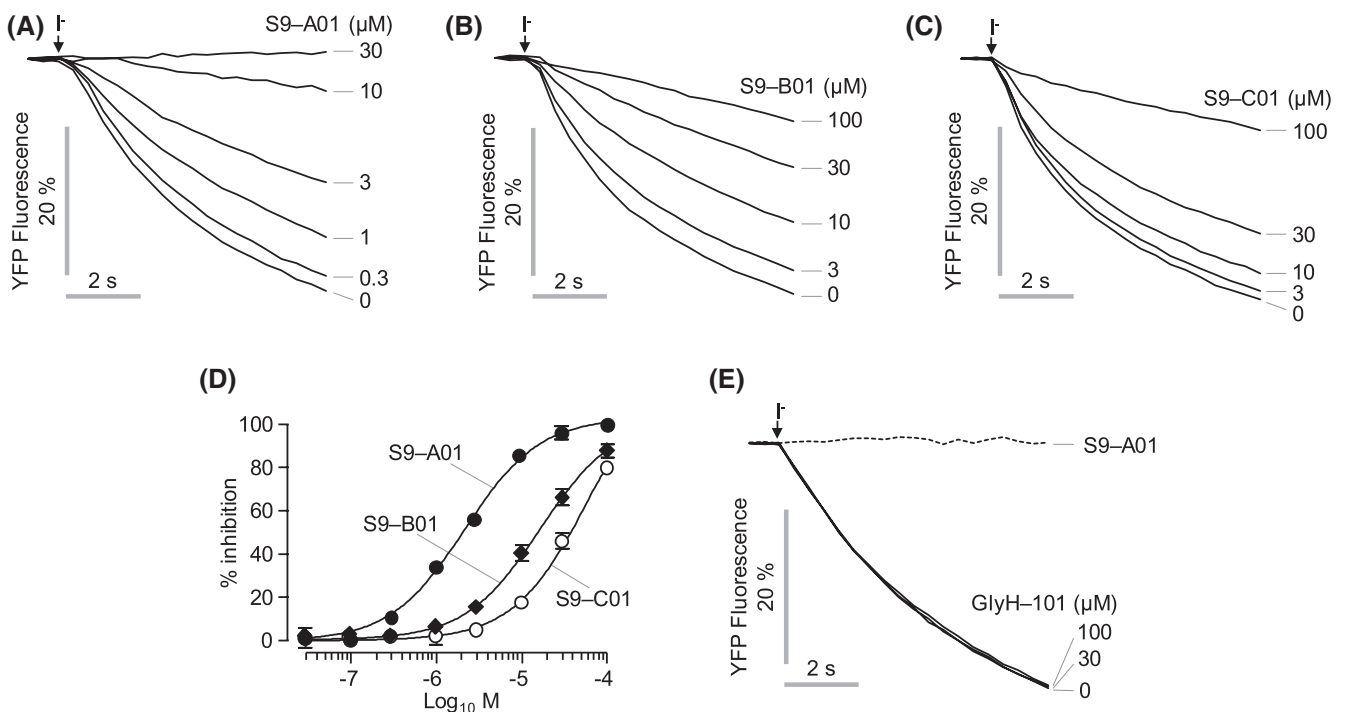


FIGURE 2 Effect of S9-A01, S9-B01, and S9-C01 on the Cl^-/I^- exchange activity of SLC26A9. (A–C) Inhibitory effect of S9-A01, S9-B01, and S9-C01 on SLC26A9-mediated Cl^-/I^- exchange observed in YFP halide-quenching assays with LN215-SLC26A9-YFP cells. The indicated concentrations of S9-A01, S9-B01, and S9-C01 were used to pretreat for 10 min prior to iodide injection. (D) Dose-response curves for S9-A01, S9-B01, and S9-C01. Mean \pm SEM ($n = 4-6$). (E) LN215-SLC26A9-YFP cells were pretreated with the indicated concentrations of GlyH-101 and S9-A01 (30 μ M) for 10 min prior to iodide injection. Mean \pm SEM ($n = 4-6$).

TABLE 2 Effect of S9-A01 derivatives (Cmpd) on Cl⁻/I⁻ exchange activity of SLC26A9

Cmpd	R1	R2	IC ₅₀ (μM)	Cmpd	R1	R2	IC ₅₀ (μM)
S9-A01		CH ₂ CH ₃	2.25 ± 0.52	S9-A10		Cl	3.68 ± 0.92
S9-A02		H	>30	S9-A11		CH ₂ CH ₃	>30
S9-A03		CH ₃	0.28 ± 0.04	S9-A12		CH ₂ CH ₃	1.08 ± 0.89
S9-A04		Cl	0.11 ± 0.02	S9-A13		CH ₃	0.09 ± 0.01
S9-A05		CH ₃	>30	S9-A14		CH ₂ CH ₃	>30
S9-A06		Cl	>30	S9-A15		CH ₂ CH ₃	>30
S9-A07		CH ₃	0.58 ± 0.04	S9-A16		H	>30
S9-A08		Cl	0.10 ± 0.02	S9-A17		CH ₂ CH ₃	>30
S9-A09		CH ₃	>30	S9-A18		CH ₃	0.26 ± 0.01

Note: IC₅₀ values were determined using YFP fluorescence quenching assay in LN215-SLC26A9-YFP cells (mean ± S.E., n = 3).

S9-A13 in a dose-dependent manner (Figure 5C–F). Currents in mock-transfected cells were not affected by S9-A13. Moreover, CFTR currents were only marginally inhibited at the highest concentration of S9-A13 (5 μM), and only at strongly depolarized clamp voltages (Figure 5G,H). Notably, SLC26A9 currents were not further stimulated by increase in intracellular cAMP using IBMX/forskolin (Figure 5I).

3.5 | S9-A13 has a minor effect on ion transport in human airway epithelial cells

We analyzed the effects of S9-A13 in BCI-NS1 human airway epithelial cells, which strongly express CFTR.²⁵ These cells also express a number of SLC26A9 splice variants, leading to isoform a (87 kDa; NM_052934.4), b (97.3 kDa; NM_134325.3), x1 (77 kDa;

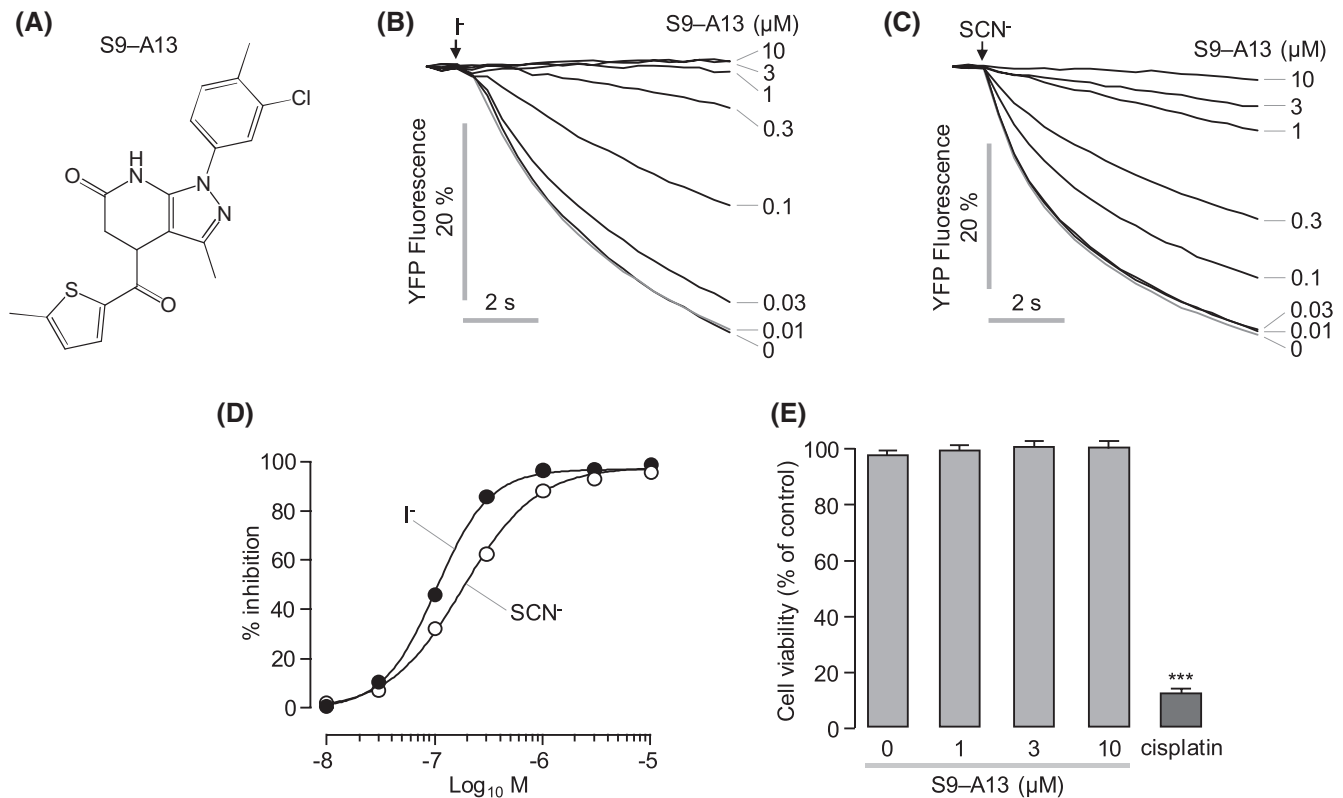


FIGURE 3 Effect of S9-A13 on SLC26A9-mediated Cl^-/base exchange activity. (A) Chemical structure of S9-A13. (B and C) SLC26A9-mediated Cl^-/I^- and Cl^-/SCN^- exchange activities were measured in LN215-SLC26A9-YFP cells. Indicated concentrations of S9-A13 were pretreated for 10 min. (D) S9-A13 dose–response for the inhibition of SLC26A9-mediated Cl^-/I^- and Cl^-/SCN^- exchange activity. Mean \pm SEM ($n = 5$). *Significant activation by IF ($p < .05$; paired t -test). (E) Effect of S9-A13 on cell viability in Calu-3 cells. Cells were treated with S9-A13 for 24 h; cell viability was determined by MTS colorimetric assay. Mean \pm SEM ($n = 6$).

XM_011509121.2), $\times 2$ (68.9 kDa; XM_011509122.2), and $\times 3$ (51 kDa; XM_011509124.2)¹⁸ (Figure 6A, Figure S1). The same pattern for SLC26A9 variants was detected in other human airway epithelial cell lines, such as Calu3 or CFBE140- (not shown). The larger band size for SLC26A9 in airways of about 120 kDa is most likely due to glycosylation,⁴ while overexpression of SLC26A9 in HEK293 cells produced a band at only around 90 kDa (Figure 5A). Immunostaining of SLC26A9 in plastic grown BCI-NS1 cells demonstrated intracellular and plasma membrane localization (Figure 6B). Surprisingly, S9-A13-inhibitable Cl^- currents were not detected, suggesting no Cl^- transport by SLC26A9 in normal airways. (Figure 6C).

BCi-NS1 cells were grown on permeable supports in PneumaCult™ differentiation media under ALI. BCI-NS1 formed a well differentiated epithelium with mostly ciliated epithelial cells (Figure 7A). The effects of S9-A13 on short circuit currents were examined in Ussing chamber recordings. We found a small albeit significant inhibition of basal I_{sc} by increasing concentrations of S9-A13 (Figure 7B,C). However, when compared to the pronounced inhibition of IF-activated I_{sc}

by $\text{CFTR}_{\text{inh-172}}$ (CFinh), inhibition of I_{sc} by S9-A13 was negligible. In BCI-NS1 airway cells, $\text{CFTR}_{\text{inh-172}}$ inhibited also basal I_{sc} present under non-stimulated conditions (Figure S4C-E). Essentially identical results were obtained in primary human airway epithelial cells (Figure S4A,B). The results indicate that CFTR is in charge of both basal and stimulated Cl^- secretion in human airways.

3.6 | Basal transport in mouse trachea is due to CFTR but not Slc26a9

We also examined expression of Slc26a9, constitutive transport (I_{sc} ; measured under open circuit conditions) and inhibition by S9-A13 in freshly excised mouse tracheas. Immunohistochemistry demonstrated apical expression of Slc26a9 in ciliated cells of mouse airway epithelium, while non-ciliated cells such as club cells and goblet cells did not express SLC26A9 (Figure 8A). S9-A13 did not inhibit constitutive (basal) ion transport in mouse trachea (Figure 8B,C). In contrast, $\text{CFTR}_{\text{inh-172}}$ dose dependently blocked basal I_{sc} , again demonstrating CFTR

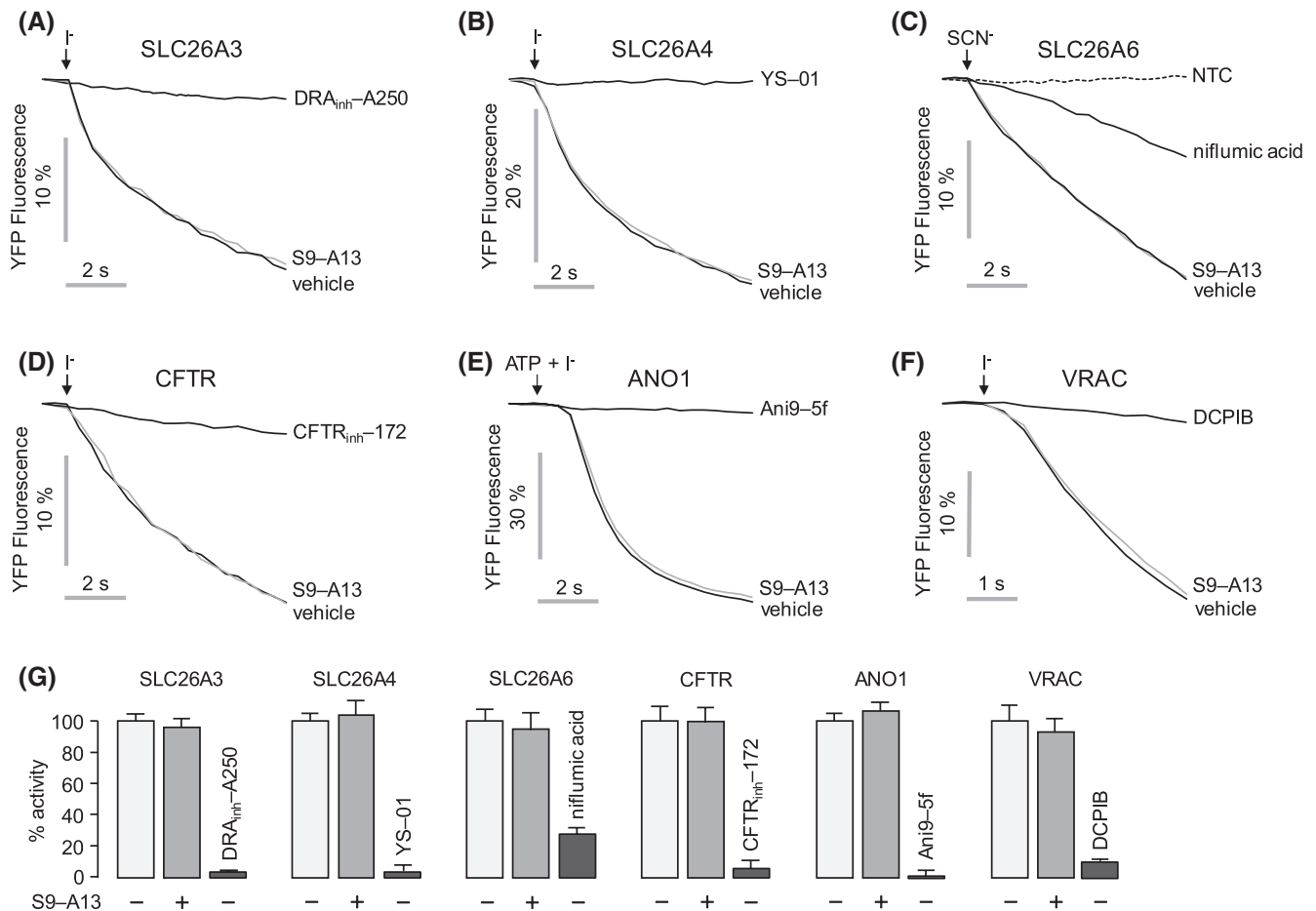


FIGURE 4 Effect of S9-A13 does not inhibit other SLC26 family members or chloride channels. (A–C) Effects of S9-A13 on Cl^-/I^- exchange activities by SLC26A3, SLC26A4, and SLC26A6 were measured using a YFP fluorescence quenching assay. Cells were pretreated with 10 μM of S9-A13 (gray line) for 10 min. SLC26A3, SLC26A4, and SLC26A6 were inhibited by $\text{DRA}_{\text{inh}}\text{-A250}$ (10 μM), YS-01 (10 μM), and niflumic acid (500 μM), respectively. (D–F) Effects of S9-A13 on CFTR, ANO1, and VRAC measured by YFP quenching in FTR-CFTR-YFP, FTR-ANO1-YFP, and LN215-YFP cells. CFTR was activated by 10 μM forskolin. ANO1 was activated by 100 μM ATP. CFTR and ANO1 were inhibited by $\text{CFTR}_{\text{inh}}\text{-172}$ (10 μM) and Ani9-5f (10 μM), respectively. VRAC was activated by a hypotonic challenge and was inhibited by 30 μM DCPIB. (G) Summary of the results obtained in A–F. Mean \pm SEM ($n = 4\text{--}5$).

as constitutive Cl^- conductance in airways (Figure 8D,E). In contrast to Ca^{2+} -dependent (Tmem16a) Cl^- secretion (ATP), cAMP activated transport (CFTR; IF) was small, due to low expression of CFTR in mouse trachea.²⁹ The small activation of I_{sc} by IF in the presence of $\text{CFTR}_{\text{inh}}\text{-172}$, is explained by activation of $\text{KCNQ1}/\text{KCNE3}$ K^+ channels.³⁰

3.7 | SLC26A9 supports alkalization of ASL pH and H^+ secretion by gastric cells

Because we found little contribution of SLC26A9 to Cl^- transport, we examined if SLC26A9 has a different function in airways. In ASL pH measurements, fully differentiated nasal epithelial cells were exposed to S9-A13

or control solution. Online recordings of ASL pH under thin film conditions indeed showed a sustained decrease in ASL pH by S9-A13. (Figure 9A–D). Two hours after application of S9-A13, ASL pH dropped by 0.23 ± 0.11 ($n = 6$) units. Subsequent stimulation of CFTR by forskolin caused only a small but not significant increase in ASL pH in airways exposed to S9-A13. These results strongly suggest a role of SLC26A9 for alkalization of ASL pH.

As SLC26A9 was proposed as apical Cl^- transporter relevant for HCl secretion by gastric parietal cells,⁶ we also examined the effect of S9-A13 on histamine-induced H^+ secretion by HGT-1 human gastric cells. Remarkably, S9-A13 significantly inhibited H^+ secretion by HGT-1 cells, supporting the concept of SLC26A9 being a Cl^- release channel in parietal cells^{5,6,19} (Figure 9E).

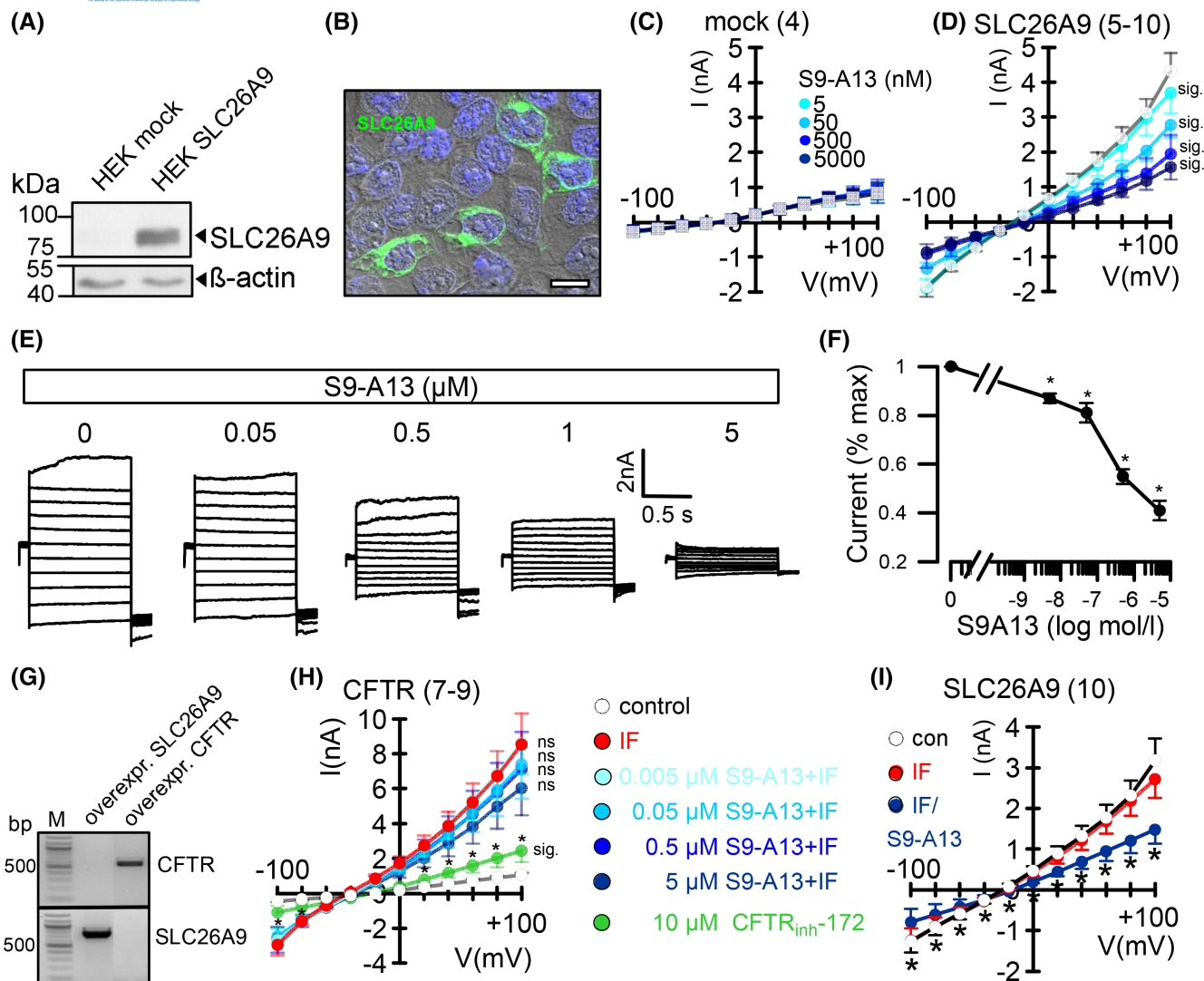


FIGURE 5 S9-A13 inhibits SLC26A9 currents in HEK293 cells. (A and B) Western blot and immunolabeling of SLC26A9 expressed in HEK293 cells demonstrating partial membrane expression of SLC26A9. Bar = 20 μm . (C) Current/voltage relationships for whole cell currents obtained in mock-transfected HEK293 cells, demonstrating absence of basal currents and lack of S9-A13 effects. (D) Enhanced basal ion currents in cells expressing SLC26A9, which are inhibited dose dependently by S9-A13. (E) Overlays of SLC26A9 currents showing inhibition by S9-A13. (F) Corresponding concentration-response curve. (G) RT-PCR showing overexpression of SLC26A9 and CFTR in HEK293 cells. (H) Lack of inhibition of CFTR whole cell currents (IBMX and forskolin, IF; 100 μM and 2 μM) by S9-A13. Only the highest concentration of S9-A13 (5 μM) inhibited currents at +100 mV clamp voltages, while CFTR_{inh}-172 (10 μM) strongly inhibited CFTR currents. (I) Inhibition of SLC26A9 by S9-A13 and lack of further activation of SLC26A9 by IF. Mean \pm SEM (number of cells). *Significant inhibition by S9-A13 and CF_{inh}172 (10 μM) ($p < .05$; paired t -test).

4 | DISCUSSION

In the present study, we demonstrate S9-A13 as the first specific and highly potent inhibitor of SLC26A9. S9-A13 inhibits SLC26A9 in the low nanomolar range. It does not show cytotoxic effects, even at micromolar concentrations. The inhibitor was used to examine the potential role of SLC26A9 for ion transport in the airway epithelium. This is of particular interest in cystic fibrosis, as genome-wide association studies demonstrated SLC26A9 as an important modifier of CF lung and gastrointestinal

disease: (i) SLC26A9 is expressed in the intestinal and airway epithelium as well as other CF-relevant tissues, (ii) single nucleotide polymorphisms (cSNPs) of SLC26A9 were found to be associated with variable anion transport properties, and (iii) SLC26A9 was shown to modulate CF-related intestinal disease, diabetes and airway response to CFTR-therapeutics.³¹⁻³⁵

A number of studies argue in favor of CFTR being responsible for constitutive (basal) anion secretion that is absent in CF airways.^{26,36,37,38} Other reports provided evidence for the role of SLC26A9 in basal airway

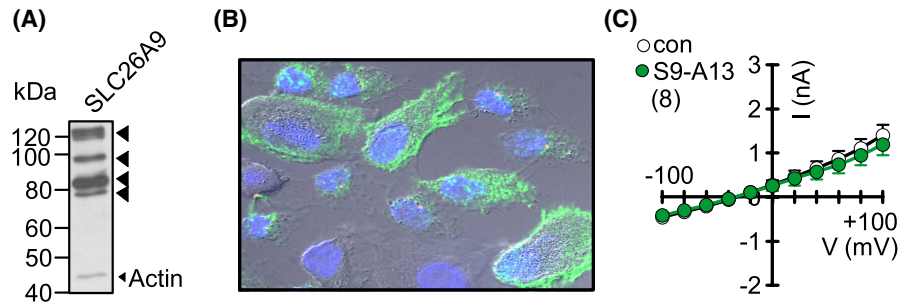


FIGURE 6 Endogenous SLC26A9 in BCI-NS1 human airway epithelial cells does not produce a Cl^- current. (A) Western blot indicates expression of various isoforms of SLC26A9. (B) Immunocytochemistry of SLC26A9 in nonpolarized BCI-NS1 cells. (C) Current/voltage relationships showing no effect S9-A13 (5 μM) on constitutive currents. Mean \pm SEM (number of cells).

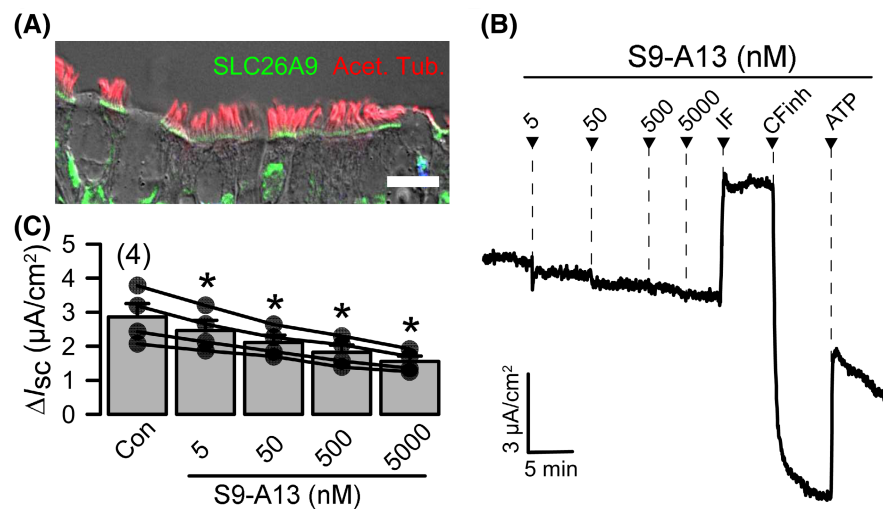


FIGURE 7 Minimal contribution of SLC26A9 to basal ion transport in differentiated BCI-NS1 airway epithelial cells. (A) Pseudostratified ciliated airway epithelium formed by differentiated BCI-NS1 cells. Immunohistochemistry indicates apical expression of SLC26A9 in ciliated cells. Bar = 10 μm . (C and D) Small but significant concentration-dependent inhibition of basal short circuit currents by S9-A13 (I_{sc} ; presence of amiloride). Increasing concentrations of S9-A13 were added subsequently to the chamber. Activation of CFTR by IF (100 μM /2 μM) and inhibition by CFTR_{inh}-172 (CFinh; 20 μM) was dominating when compared to the effects of S9-A13. ATP was applied at 100 μM . Mean \pm SEM (number of tissues). *Significant inhibition of I_{sc} ($p < .05$; paired t -test).

Cl^- transport.^{4,7,11,39,40} So far it was difficult to discriminate between both conductances due to the lack of specific inhibitors for SLC26A9. SLC26A9 inhibitors used in earlier studies were not specific and inhibited also other Cl^- channels.^{1,2,4} Moreover, expression and activity of both CFTR and SLC26A9 are functionally connected. Intracellular trafficking and constitutive activity of SLC26A9 are compromised in cystic fibrosis (CF) airway epithelia expressing the trafficking mutant F508del-CFTR.⁴⁰⁻⁴² In the presence of F508del-CFTR, binding of the PDZ-domain protein CAL inhibits the function of SLC26A9 due to enhanced endoplasmic reticulum-associated proteasomal degradation.⁴³ Vice versa, SLC26A9 may support biogenesis and/or stabilization of CFTR.⁴⁴

Here we present evidence that SLC26A9 is located in the apical membrane of ciliated airway epithelial cells, but

not in non-ciliated club or goblet cells. Overexpression of SLC26A9 induced a basal Cl^- conductance in HEK293 cells, which was well inhibited by S9-A13. Unlike reported recently,³⁹ SLC26A9 in HEK293 cells could not be further activated by increase in intracellular cAMP (Figure 5I). SLC26A9 is expressed endogenously in human airway epithelial cells such as CFBE, Calu3, and BCI-NS1, but Cl^- transport by SLC26A9 could not be detected in these cells using S9-A13. As airways express CFTR, we speculate regulation of SLC26A9 mediated HCO_3^- transport by CFTR.

Evidence for a role of SLC26A9 in HCO_3^- transport was presented earlier.^{3,5,6,19,45,46} Other studies detected transport of Cl^- but not HCO_3^- by SLC26A9.^{1,2,4,8} pH measurements in HEK293 cells expressing SLC26A9 did not provide conclusive evidence for SLC26A9-mediated HCO_3^- transport (Figure S2). In CFTR-expressing BCI-NS1 cells, primary human

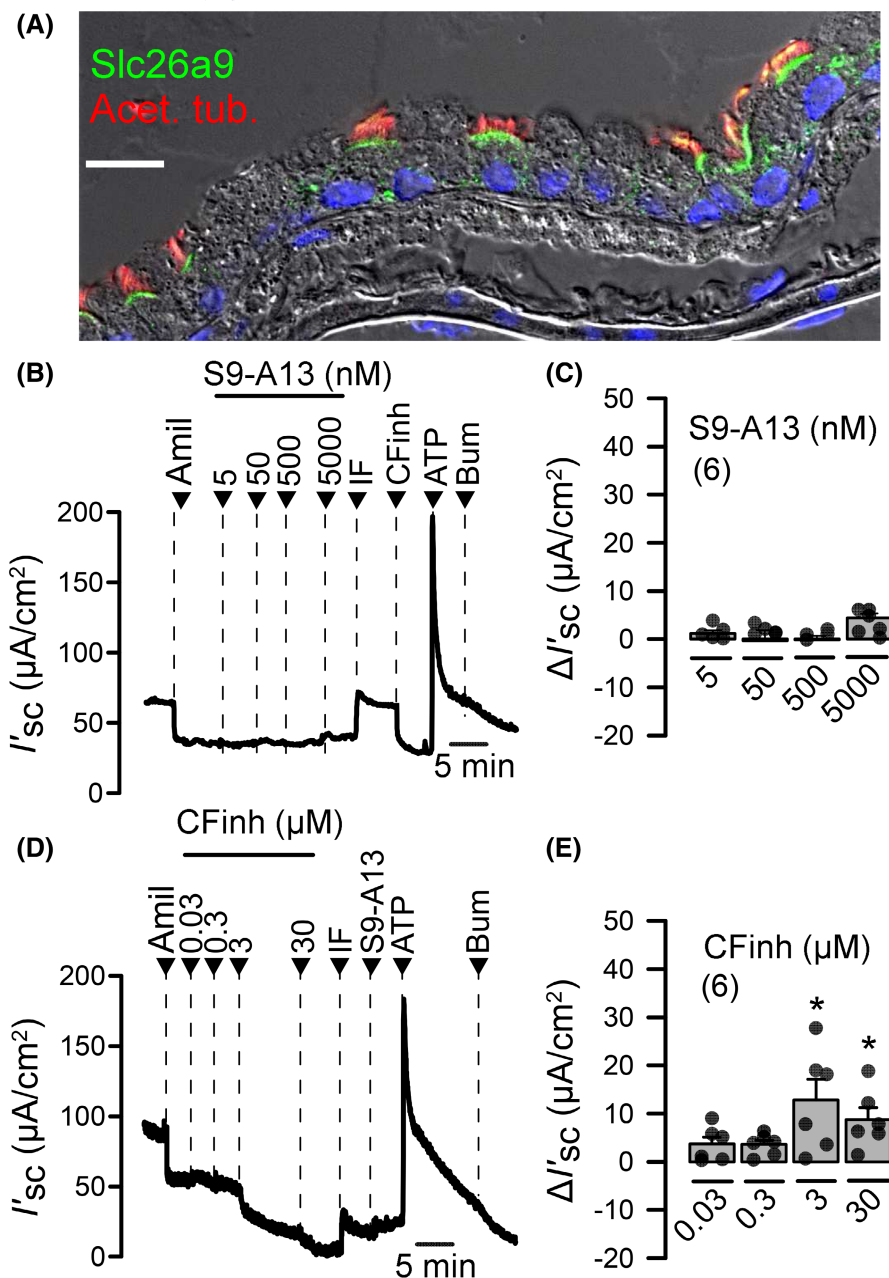


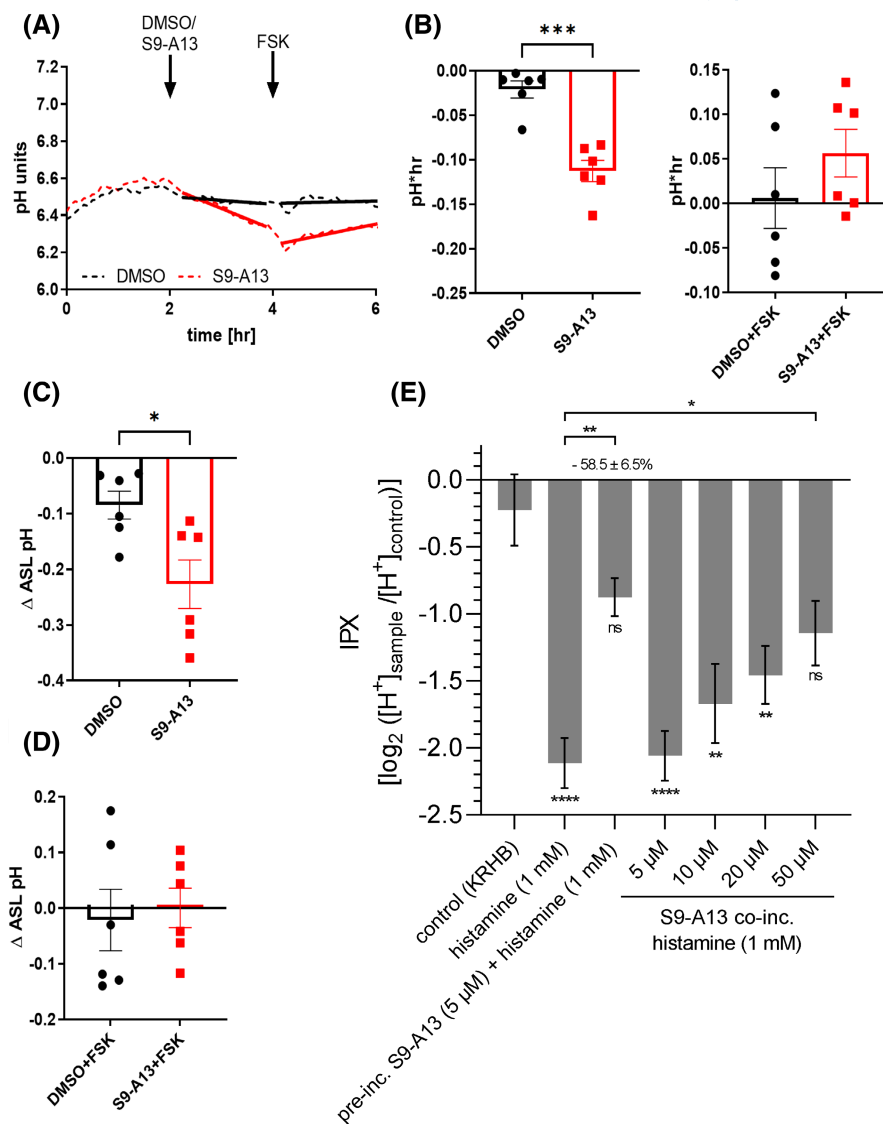
FIGURE 8 Basal ion transport in mouse trachea is due to CFTR but not SLC26A9. (A) Airway epithelium from mouse trachea. Immunohistochemistry indicates apical expression of SLC26A9 in ciliated airway epithelial cells. Bar = 20 μm . (B and C) Constitutive equivalent short circuit current (I_{sc}) assessed in open circuit Ussing chamber recordings, were not inhibited by S9-A13. (D and E) Concentration dependent inhibition of constitutive I_{sc} by CFTR_{inh}-172. Mean \pm SEM (number of tracheas). *Significant inhibition of I_{sc} ($p < .05$; paired t -test).

airway epithelial cells and mouse trachea a substantial SLC26A9-mediated Cl^- transport could not be detected (Figures 6–8, Figure S4). In contrast, airway surface liquid pH was significantly reduced by S9-A13, suggesting a role of SLC26A9 for HCO_3^- secretion (Figure 9A–D).

In cells that only express SLC26A9 but not CFTR such as HEK293 cells or LN215 cells, Cl^-/HCO_3^- exchange by SLC26A9 could not be detected, while Cl^- transport by SLC26A9 is clearly present (Figures 1–3, and 5, Figure S3). Stomach mucosa expresses only low levels of CFTR,⁴⁷ Here SLC26A9-mediated Cl^- transport may parallel H^+ secretion by the proton pump. This is supported by S9-A13-dependent inhibition of H^+ secretion in HGT-1 human gastric cells^{5,6,19} (Figure 9). We speculate

that depending on expression of CFTR, SLC26A9 may transport Cl^- or HCO_3^- .³ While Cl^- secretion is due to CFTR, basal HCO_3^- secretion might be due to SLC26A9 (Figure 8, Figure S4C,D). Immunofluorescence suggested pronounced expression in ciliated cells, while transcriptome analysis indicated SLC26A9 enriched in pulmonary neuroendocrine cells, where it could have sensory, neuroendocrine or other functions to protect airways from mucus obstruction. Interestingly, even in the presence of the inhibitor of adenylate cyclase type 1, ST034307, or in the presence of the adenosine 2AB inhibitor PSB603, basal Cl^- secretion by CFTR is still detectable (Figure S4E). This suggests that CFTR does not need to be activated by cAMP/PKA to produce a basal Cl^- conductance, but may be activated by SLC26A9.⁴⁴ The novel SLC26A9 inhibitor

FIGURE 9 SLC26A9 supports alkalinization of ASL pH and H^+ secretion by gastric cells. (A) Real-time ASL pH traces showing response to addition of S9-A13 (5 μ M) or control (DMSO) and subsequent stimulation with forskolin (FSK; 10 μ M). (B) Rate of ASL pH change per hour after adding S9-A13 or control (left) and rate of pH change after adding FSK (right). (C) Absolute change in ASL pH after adding S9-A13 or control. (D) Absolute change in ASL pH after adding FSK. Mean \pm SEM ($n = 6$). *Significant inhibition of Isc ($p < .05$; paired t -test). (E) Summary of the inhibitory effects of S9-A13 (30 min preincubation or 10 min coincubation) on proton secretion by HGT-1 human gastric cells stimulated with histamine (1 mM). Mean \pm SEM ($n = 4-6$). *Significant difference ($p < .05-.0001$; one-way ANOVA & Holm-Šidák post hoc test).



S9-A13 may allow to further unravel functional relationships between CFTR and SLC26A9.

AUTHOR CONTRIBUTIONS

Sungwoo Jo, Raquel Centeio, Jiraporn Ousingsawat, Khaoula Talbi, Kunhi Ryu, Livia Delpiano, Violeta Railean, Lisa W. Rodenburg, Karl Kunzelmann, and Jinhong Park performed the experiments and analyzed data. Rainer Schreiber and Sungwoo Jo performed molecular biology. Wan Namkung, Kristin Kahlenberg, Sungwoo Jo, Raquel Centeio, Jiraporn Ousingsawat, Khaoula Talbi, Kunhi Ryu, Veronika Somoza, Mike A. Gray, Margarida D. Amaral, Jeffrey M. Beekman, and Jinhong Park designed the study. Wan Namkung, Karl Kunzelmann, Sungwoo Jo, and Raquel Centeio interpreted data and drafted the manuscript.

ACKNOWLEDGMENTS

This study was supported by UK CF Trust SRC013, DFG KU756/14-1, Gilead Stiftung, and National Research

Foundation of Korea (NRF2018R1A6A1A03023718 and NRF2020R1C1C1008332). The technical assistance by Patricia Seeberger is greatly appreciated.

DATA AVAILABILITY STATEMENT

The data that support the findings of this study are available from the corresponding author upon request.

DISCLOSURES

The authors declare no conflict of interest.

INSTITUTIONAL REVIEW BOARD STATEMENT

All animal experiments complied with the reporting of in vivo experiments guidelines and were carried out in accordance with the United Kingdom Animals Act, 1986, and associated guidelines, and EU Directive 2010/63/EU for animal experiments. All animal experiments were approved by the local Ethics Committee of the Government of Unterfranken/Wurzburg (AZ: 55.2-2532-2-1359-15)

and were conducted according to the guidelines of the American Physiologic Society and German Law for the Welfare of Animals.

ORCID

Karl Kunzelmann  <https://orcid.org/0000-0001-6222-4593>

REFERENCES

- Dorwart MR, Shcheynikov N, Wang Y, Stippec S, Muallem S. SLC26A9 is a Cl⁻ channel regulated by the WNK kinases. *J Physiol*. 2007;584:333-345.
- Loriol C, Dulong S, Avella M, et al. Characterization of SLC26A9, facilitation of Cl⁻ transport by bicarbonate. *Cell Physiol Biochem*. 2008;22:15-30.
- Chang MH, Plata C, Zandi-Nejad K, et al. Slc26a9-anion exchanger, channel and Na⁺ transporter. *J Membr Biol*. 2009;228:125-140.
- Bertrand CA, Zhang R, Pilewski JM, Frizzell RA. SLC26A9 is a constitutively active, CFTR-regulated anion conductance in human bronchial epithelia. *J Gen Physiol*. 2009;133:421-438.
- Liu X, Li T, Riederer B, et al. Loss of Slc26a9 anion transporter alters intestinal electrolyte and HCO₃⁻ transport and reduces survival in CFTR-deficient mice. *Pflugers Arch*. 2015;467:1261-1275.
- Xu J, Song P, Miller ML, et al. Deletion of the chloride transporter Slc26a9 causes loss of tubulovesicles in parietal cells and impairs acid secretion in the stomach. *Proc Natl Acad Sci U S A*. 2008;105:17955-17960.
- Larsen MB, Choi JJ, Wang X, Myerburg MM, Frizzell RA, Bertrand CA. Separating the contributions of SLC26A9 and CFTR to anion secretion in primary human bronchial epithelia (HBE). *Am J Physiol Lung Cell Mol Physiol*. 2021;321:L1147-L1160.
- Walter JD, Sawicka M, Dutzler R. Cryo-EM structures and functional characterization of murine Slc26a9 reveal mechanism of uncoupled chloride transport. *Elife*. 2019;8:e46986.
- Ballard ST, Taylor AE. Bioelectric properties of proximal bronchiolar epithelium. *Am J Physiol*. 1994;267:L79-L84.
- Al-Bazzaz FJ. Regulation of Na and Cl transport in sheep distal airways. *Am J Physiol*. 1994;267:L193-L198.
- Ousingsawat J, Schreiber R, Kunzelmann K. Differential contribution of SLC26A9 to Cl⁻ conductance in polarized and non-polarized epithelial cells. *J Cell Physiol*. 2011;227:2323-2329.
- Ko SB, Shcheynikov N, Choi JY, et al. A molecular mechanism for aberrant CFTR-dependent HCO₃⁻ transport in cystic fibrosis. *EMBO J*. 2002;21(21):5662-5672.
- Ko SB, Zeng W, Dorwart MR, et al. Gating of CFTR by the STAS domain of SLC26 transporters. *Nat Cell Biol*. 2004;6:343-350.
- Rakonczay Z Jr, Hegyi P, Hasegawa M, et al. CFTR gene transfer to human cystic fibrosis pancreatic duct cells using a Sendai virus vector. *J Cell Physiol*. 2008;214:442-455.
- Rode B, Dirami T, Bakouh N, et al. The testis anion transporter TAT1 (SLC26A8) physically and functionally interacts with the cystic fibrosis transmembrane conductance regulator channel: a potential role during sperm capacitation. *Hum Mol Genet*. 2012;21:1287-1298.
- El Khouri E, Toure A. Functional interaction of the cystic fibrosis transmembrane conductance regulator with members of the SLC26 family of anion transporters (SLC26A8 and SLC26A9): physiological and pathophysiological relevance. *Int J Biochem Cell Biol*. 2014;52:58-67.
- Chang MH, Plata C, Sindic A, et al. Slc26a9 is inhibited by the R-region of CFTR via the STAS domain. *J Biol Chem*. 2009;284:28306-28318.
- Xu J, Henriksnäs J, Barone S, et al. SLC26A9 is expressed in gastric surface epithelial cells, mediates Cl⁻/HCO₃⁻ exchange, and is inhibited by NH₄⁺. *Am J Physiol Cell Physiol*. 2005;289:C493-C505.
- Demitrack ES, Soleimani M, Montrose MH. Damage to the gastric epithelium activates cellular bicarbonate secretion via SLC26A9 Cl⁻/HCO₃⁻. *Am J Physiol Gastrointest Liver Physiol*. 2010;299:G255-G264.
- Schreiber R, Castrop H, Kunzelmann K. Allergen induced airway hyperresponsiveness is absent in ecto-5'-nucleotidase (CD73) deficient mice. *Pflugers Arch*. 2008;457:431-440.
- Park J, Lee HJ, Song D, et al. Novel pendrin inhibitor attenuates airway hyperresponsiveness and mucin expression in experimental murine asthma. *J Allergy Clin Immunol*. 2019;144:1425-1428.e1412.
- Besteman SB, Phung E, Raeven HHM, et al. Recurrent respiratory syncytial virus infection in a CD14 deficient patient. *J Infect Dis*. 2022;226:258-269.
- Holik AK, Schweiger K, Stoeger V, et al. Gastric serotonin biosynthesis and its functional role in L-arginine-induced gastric proton secretion. *Int J Mol Sci*. 2021;22:5881.
- Ousingsawat J, Centeio R, Schreiber R, Kunzelmann K. Expression of SLC26A9 in airways and its potential role in asthma. *Int J Mol Sci*. 2022;23:2998.
- Cabrita I, Benedetto R, Wanitchakool P, et al. TMEM16A mediated mucus production in human airway epithelial cells. *Am J Respir Cell Mol Biol*. 2020;64:50-58.
- Benedetto R, Centeio R, Ousingsawat J, Schreiber R, Janda M, Kunzelmann K. Transport properties in CFTR^{-/-} knockout piglets suggest normal airway surface liquid pH and enhanced amiloride-sensitive Na⁺ absorption. *Pflugers Arch*. 2020;472:1507-1519.
- Centeio R, Ousingsawat J, Schreiber R, Kunzelmann K. CLCA1 regulates airway mucus production and ion secretion through TMEM16A. *Int J Mol Sci*. 2021;22:5133.
- Saint-Criq V, Haq IJ, Gardner AI, et al. Real-time, semi-automated fluorescent measurement of the airway surface liquid pH of primary human airway epithelial cells. *J Vis Exp*. 2019;13. doi:10.3791/59815
- Rochelle LG, Li DC, Ye H, Lee E, Talbot CR, Boucher RC. Distribution of ion transport mRNAs throughout murine nose and lung. *Am J Physiol*. 2000;279:L14-L24.
- Preston P, Wartosch L, Gunzel D, et al. Disruption of the K⁺ channel beta-subunit KCNE3 reveals an important role in intestinal and tracheal Cl⁻ transport. *J Biol Chem*. 2010;285:7165-7175.
- Chen AP, Chang MH, Romero MF. Functional analysis of nonsynonymous single nucleotide polymorphisms in human SLC26A9. *Hum Mutat*. 2012;33:1275-1284.
- Sun L, Rommens JM, Corvol H, et al. Multiple apical plasma membrane constituents are associated with susceptibility to meconium ileus in individuals with cystic fibrosis. *Nat Genet*. 2012;44:562-569.

33. Miller MR, Soave D, Li W, et al. Variants in solute carrier SLC26A9 modify prenatal exocrine pancreatic damage in cystic fibrosis. *J Pediatr*. 2015;166:1152-1157.e1156.
34. Lam AN, Aksit MA, Vecchio-Pagan B, et al. Increased expression of anion transporter SLC26A9 delays diabetes onset in cystic fibrosis. *J Clin Invest*. 2020;130:272-286.
35. Strug LJ, Gonska T, He G, et al. Cystic fibrosis gene modifier SLC26A9 modulates airway response to CFTR-directed therapeutics. *Hum Mol Genet*. 2016;25:4590-4600.
36. Ishibashi K, Okamura K, Yamazaki J. Involvement of apical P2Y2 receptor-regulated CFTR activity in muscarinic stimulation of Cl⁻ reabsorption in rat submandibular gland. *Am J Physiol Regul Integr Comp Physiol*. 2008;294:R1729-R1736.
37. Wang X, Lytle C, Quinton PM. Predominant constitutive CFTR conductance in small airways. *Respir Res*. 2005;6:7.
38. Song Y, Salinas D, Nielson DW, Verkman AS. Hyperacidity of secreted fluid from submucosal glands in early cystic fibrosis. *Am J Physiol Cell Physiol*. 2006;290:C741-C749.
39. Salomon JJ, Spahn S, Wang X, Fullekrug J, Bertrand CA, Mall MA. Generation and functional characterization of epithelial cells with stable expression of SLC26A9 Cl⁻ channels. *Am J Physiol Lung Cell Mol Physiol*. 2016;310:L593-L602.
40. Bertrand CA, Mitra S, Mishra SK, et al. The CFTR trafficking mutation F508del inhibits the constitutive activity of SLC26A9. *Am J Physiol Lung Cell Mol Physiol*. 2017;312:L912-L925.
41. Sato Y, Thomas DY, Hanrahan JW. The anion transporter SLC26A9 localizes to tight junctions and is degraded by the proteasome when co-expressed with F508del-CFTR. *J Biol Chem*. 2019;294:18269-18284.
42. Pinto MC, Quaresma MC, Silva IAL, Railean V, Ramalho SS, Amaral MD. Synergy in cystic fibrosis therapies: targeting SLC26A9. *Int J Mol Sci*. 2021;22:13064.
43. Needham PG, Goeckeler-Fried JL, Zhang C, et al. SLC26A9 is selected for endoplasmic reticulum associated degradation (ERAD) via Hsp70-dependent targeting of the soluble STAS domain. *Biochem J*. 2021;478:4203-4220.
44. Avella M, Loriol C, Boulukos K, Borgese F, Ehrenfeld J. SLC26A9 stimulates CFTR expression and function in human bronchial cell lines. *J Cell Physiol*. 2011;226:212-223.
45. Lohi H, Kujala M, Makela S, et al. Functional characterization of three novel tissue-specific anion exchangers SLC26A7, -A8, and -A9. *J Biol Chem*. 2002;277:14246-14254.
46. Simão S, Gomes P, Pinho MJ, Soares-da-Silva P. Identification of SLC26A transporters involved in the Cl⁻/HCO₃⁻ exchange in proximal tubular cells from WKY and SHR. *Life Sci*. 2013;93:435-440.
47. Strong TV, Boehm K, Collins FS. Localization of cystic fibrosis transmembrane conductance regulator mRNA in the human gastrointestinal tract by in situ hybridization. *J Clin Invest*. 1994;93:347-354.

SUPPORTING INFORMATION

Additional supporting information can be found online in the Supporting Information section at the end of this article.

How to cite this article: Jo S, Centeio R, Park J, et al. The SLC26A9 inhibitor S9-A13 provides no evidence for a role of SLC26A9 in airway chloride secretion but suggests a contribution to regulation of ASL pH and gastric proton secretion. *The FASEB Journal*. 2022;36:e22534. doi:[10.1096/fj.202200313RR](https://doi.org/10.1096/fj.202200313RR)